Electrical signature of nanoscale coalescence in a percolating Bi nanocluster film

P. Y. Convers,[1] D. N. McCarthy,[1] A. Sattar,[1] F. Natali,[1] S. C. Hendy,[2,3] and S. A. Brown[1]
[1]*MacDiarmid Institute for Advanced Materials and Nanotechnology, Department of Physics and Astronomy, University of Canterbury, Christchurch 8140, New Zealand*
[2]*MacDiarmid Institute for Advanced Materials and Nanotechnology, School of Chemical and Physical Sciences, Victoria University of Wellington, Wellington 6140, New Zealand*
[3]*Industrial Research Ltd., Lower Hutt 5040, New Zealand*
(Received 31 January 2010; revised manuscript received 10 August 2010; published 8 September 2010)

We explore changes in the electrical conductance of a percolating Bi nanocluster film due to coalescence. A power law increase in conductance is observed immediately after deposition and we show this corresponds to power law changes in the radius of the necks between clusters. The power-law exponent (≤ 0.04) is much smaller than expected from classical models of microparticle coalescence. Atomistic kinetic Monte Carlo simulations reveal similar behavior during a late stage of coalescence where faceting near the necks slows the effects of surface diffusion.

DOI: 10.1103/PhysRevB.82.115409 PACS number(s): 61.46.Bc, 64.60.ah, 73.63.−b, 81.07.Lk

Instabilities driving material rearrangement on a macroscopic scale can be witnessed everyday, for example, in the coalescence of droplets on a shower wall or the breaking of a water stream from a tap into isolated droplets (the Rayleigh instability[1]). Even solids will coalesce together, if given enough time, and it was shown by Kuczynski[2] and Nichols and Mullins[3] that the neck radius r between two coalescing microscale solid particles follows a power law

$$r \propto t^{\alpha}, \tag{1}$$

where α is specific to the physical coalescence process and lies between $\frac{1}{6}$ (surface diffusion) and $\frac{1}{2}$ (viscous flow). Since the final equilibration time is proportional to the fourth power of the particle radius,[4] both coalescence and the Rayleigh instability could have profound effects on nanoscale systems,[5] and especially on the fabrication and stability of nanoelectronic devices, such as those composed of nanoparticles.[6] It is important, therefore, to develop a detailed understanding of these effects on the nanoscale and, in particular, to establish whether the understanding of the microscale can be carried over to the nanoscale.

Experimental determination of the evolution of the neck radius of microparticles can be achieved using an optical microscope[2,7] and although it was recently shown that it is possible to observe this evolution for Au nanoparticles using electron microscopy,[8] this is much more challenging due to their small size, instability and uncontrolled heating in an electron microscope beam. A complementary and indirect method which has been used to determine the neck size between two coalescing objects is to measure the electrical conductance between them.[9] Then, in the limit of small neck radius r compared to the particle size, the conductance is given by[10]

$$G \propto r^{\omega}, \tag{2}$$

where ω is equal to 1 or 2 depending on whether r is larger or smaller than the electron mean-free path λ. Thus, Eqs. (1) and (2) suggest that the conductance is expected to follow a power law in time,

$$G \propto t^{\beta}, \tag{3}$$

where the exponent $\beta = \alpha \cdot \omega$ has a value between $\frac{1}{6}$ (surface diffusion and $\omega = 1$) and 1 (viscous flow and $\omega = 2$).

We report *in situ* measurements of the conductance of percolating bismuth nanoparticle films and use a percolation model and atomistic kinetic Monte Carlo (KMC) simulations[11] to relate the conductance of the films to the behavior of individual necks [Eqs. (1)–(3)]. The percolation model shows that coalescence of neighboring nanoparticles causes power-law behavior in the film conductance. Hence power law fits to the *experimental* data (for films) provide information about the necks, which follow Eq. (3) with $\beta \sim 0.02$. The KMC simulations demonstrate that Eqs. (1)–(3) are valid throughout the coalescence process (i.e., for all r), providing a strong link between the experimental β and the underlying value of α, which is the fundamental quantity that governs the coalescence process. The KMC simulations also show that faceting of the particles in the late stages of coalescence leads to $0.015 \lesssim \beta \lesssim 0.06$, which corresponds very well to the value $\beta \sim 0.02$ found experimentally. Hence, the coalescence of nanoparticles proceeds much more slowly than expected from the continuum model of microscale surface diffusion[2,3] and the experimentally determined value $\alpha \lesssim 0.04$ is much smaller than predicted ($\alpha \geq \frac{1}{6}$).

Bismuth nanoclusters were chosen for these experiments because of their relative ease of preparation[6] and because of the interesting properties of bismuth nanostructures.[12–14] Clusters with diameters of ~30 nm (see Fig. 1) were produced in a water-cooled inert gas aggregation source[15] (crucible temperature ~1050 K; Ar flow rate=100 sccm) and deposited under high vacuum onto SiO_2 passivated Si wafers supporting gold electrodes which monitor the conductance of the cluster film. Similar results were obtained for Pb and Sn clusters. The deposition was stopped soon after the onset of conduction, which corresponds to the percolation threshold.[6,16] The sample was at room temperature throughout the experiment; at higher temperatures the interesting coalescence processes occurred too rapidly to allow useful data to be acquired.

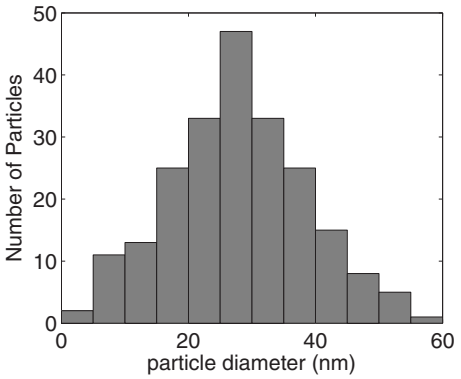

FIG. 1. Bi cluster size distribution obtained by analysis of SEM images from a low coverage (0.02ML) sample deposited with source conditions similar to those used for all other experiments reported here (crucible temperature ~1050 K; Ar flow rate =100 sccm). Low-coverage samples are required to avoid any effects of coalescence on the size distribution.

Figure 2(a) shows typical examples of the cluster film conductance after the end of deposition, which is defined as $t=0$. The changes in conductance are coincident with a change in film morphology as shown in Fig. 3. One film was

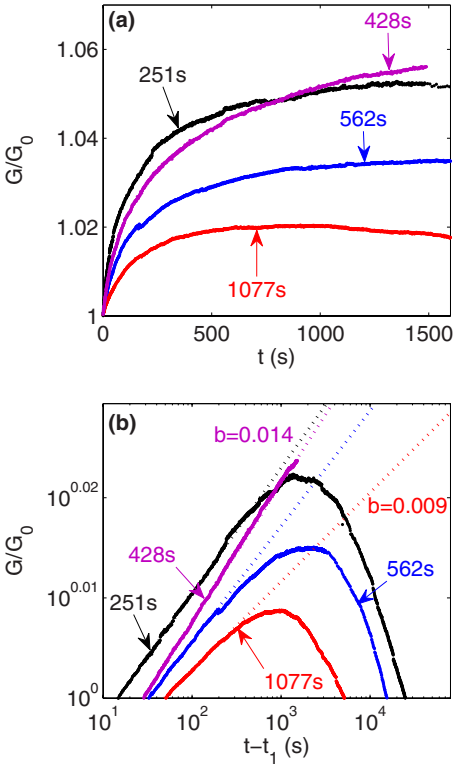

FIG. 2. (Color online) Time evolution of normalized conductance of ~0.70 ML films of ~30 nm Bi clusters deposited on a SiO_2 surface. G_0 is the conductance when the deposition is stopped, after the deposition times indicated. (a) Experimental film conductances just after deposition, for various times of deposition. (b) Same experimental conductance data as (a) on a log-log plot with shifted time scale $t-t_1$ (continuous curves) and Eq. (4) fitted between $t=0$ and 100 s (dotted curves). The extremal values of b are indicated.

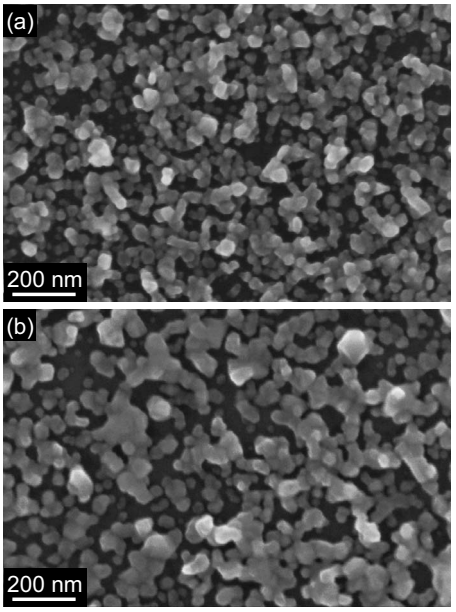

FIG. 3. SEM images of ~30 nm Bi clusters deposited on SiO_2 and exposed to air (a) immediately and (b) 3 days after deposition. The clusters are more strongly coalesced in (b).

exposed to air immediately after deposition [Fig. 3(a)], thus fixing its morphology while the other remained in vacuum for 3 days after deposition [Fig. 3(b)]. Clearly the clusters left under vacuum have coalesced more than those immediately exposed to air. The initial increase in $G(t)$ in Fig. 2(a) is driven primarily by the coalescence of neighboring particles while the reduction in $G(t)$ at longer times occurs because the cluster film (Fig. 3) evolves toward a series of isolated islands.[1,17,18] Note that the increase in conductance in Fig. 2(a), which is the focus of this paper, is less than 5%, consistent with the relatively subtle changes in film morphology observed.

The power law

$$a(t-t_1)^b \tag{4}$$

can be successfully fitted to the increase in conductance using a least square routine [see Fig. 2(b)], where a, t_1, and b are free parameters. Obviously the decrease in conductance cannot be fitted by Eq. (4), thus an upper limit of the time range used for fitting, t_{fit}, must be defined. In practice, the maximum reasonable value of t_{fit} is indicated by a sharp drop in the fit goodness parameter R^2. In the following t_{fit} =100 s, well below this maximum.

Other fit functions (for example, with fewer free parameters) have been considered[19] but were discarded because different values of t_{fit} caused the fitted parameters to vary by nearly two orders of magnitude (see discussion in Ref. 20). In the case of Eq. (4), the same range of t_{fit} causes a relatively small change in the fitted parameters, as shown in Fig. 4. Hence the experimental data are well represented by Eq. (4).

The fitted b values for the experimental data are shown in Fig. 2(b), and are summarized for all samples investigated in Fig. 5(a). For all the samples, the fitted exponent b lies in the

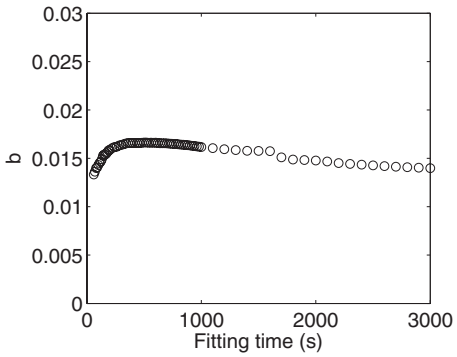

FIG. 4. Variation in the fitted exponent, b, with fitting time, t_{fit}, for a set of experimental conductance data with deposition time 568 s.

range 0.005–0.02, which is much lower than the range ($\frac{1}{6} \leq \beta \leq 1$) expected from Eq. (3), and from Refs. 2 and 3, indicating that the dominant behavior in these nanoparticle films is qualitatively different from that observed at larger scales.

It is, however, not immediately clear how the fitted exponent b (which is related to the conductance of the cluster film) is related to β (which is related to the conductance between two clusters). A complicating factor is that at the percolation threshold (or equivalently at the onset of conductance) clusters will be at varying stages of coalescence, depending on the time each individual cluster came into contact with other clusters. Thus the conductance $G(t)$ of the film is not simply proportional to the conductance $G(t)$ of one neck. To link the conductance of individual necks described by the exponent β, with the conductance of the film described by the fitted exponent b, we use a standard percolation model[6,16] in which the deposition is simulated by random occupation of sites of a two dimensional square lattice but with the additional feature that when two neighboring sites are occupied, the conductance G_i of the bond between them is given by

$$G_i(t - t_i) = \begin{cases} 0 & \text{if } t < t_i \\ (t - t_i)^{\beta} & \text{if } t \geq t_i \end{cases}, \tag{5}$$

where t_i is the time when the second site is occupied. As in the experimental depositions, the lattice is initially empty and the deposition ends (at $t=0$) when a surface coverage $\theta \sim 0.70$ is reached. In both the experiments and simulations a range of deposition rates were used so that different deposition times were required to reach the required coverage.

Typical evolutions of the modeled $G(t)$ have the same qualitative behavior as the experimental data and are also well fitted by Eq. (4) [see inset of Fig. 5(a)]. However, the modeled $G(t)$ data result from addition of a large number of exponentials and so $G(t)$ is not expected to be a simple exponential function. Therefore, it is important[20] to consider the possibility that the relationship between the fitted value of b and the underlying exponent β is dependent on both β itself and t_{fit} (as it is in the experiments—see Fig. 4 and discussion above). Figure 5(b) shows that b does in fact depend (albeit relatively weakly) on t_{fit} and that the relation $b(\beta)$ is linear for all t_{fit}. The simulations show that as long as the fitting time is not shorter than a tenth of the deposition time, β differs from b at most by a factor 2, and hence that it is possible to retrieve β by fitting Eq. (4) to $G(t)$. Therefore, when we apply the same fitting procedure to the experimental data, the value for the fitted exponent, b, can also be correlated with the exponent, β, that governs the increase in conductance between a pair of clusters. Even more importantly, for $\beta=0.02$, the deposition time dependence of the fitted parameter b for the modeled data is very similar that for the experimental data [as shown in Fig. 5(a)]. Hence the combination of fits to the modeled and experimental data lead to the conclusion that $\beta=0.02$ for the present experiments.

Assuming that Eq. (2) is valid with $\omega \geq 1$, the experimental exponent $\beta=0.02$ means that $\alpha=\frac{\beta}{\omega}$ is determined to be 0.02 at maximum. This value is inconsistent with the exponent $\alpha=\frac{1}{6}$ expected for a continuum model of surface diffusion[3] and also with the exponent $\alpha=\frac{1}{3}$ observed in atomistic simulations at small neck radius.[21,22] It is important therefore that we now investigate the possible origin of such a small exponent α, and consider in more detail the validity of Eq. (2) for large neck sizes (i.e., establish a more general relationship between the exponents α and β).

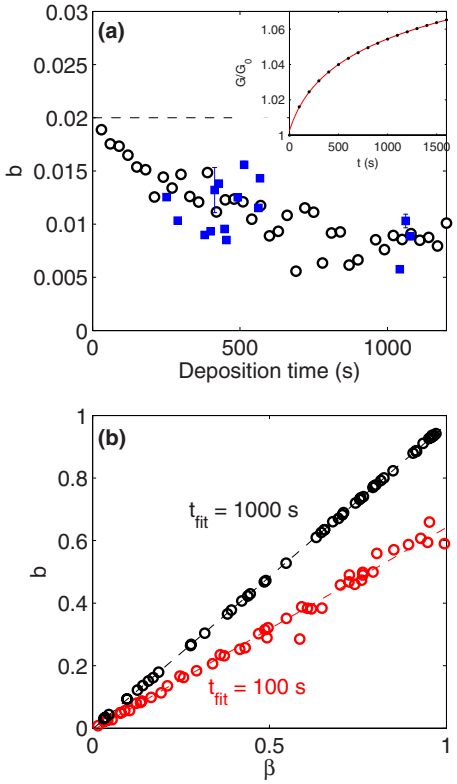

FIG. 5. (Color online) (a) Fitted exponent b as a function of deposition time ($t_{\mathrm{fit}}=100$ s). Circles are fitted exponents for modeled conductance data with $\beta=0.02$ (dashed line) and squares are fitted exponents for experimental conductance data. Inset: conductance of a simulated deposition with $t_{\mathrm{dep}}=400$ s, $\theta=0.71$, and $\beta=0.02$ (dots), fitted with Eq. (4) (continuous curve). (b) Fitted exponent b as a function of exponent β for the percolation model with $t_{\mathrm{dep}}=400$ s and $\theta=0.71$ for $t_{\mathrm{fit}}=100$ s and $t_{\mathrm{fit}}=1000$ s.

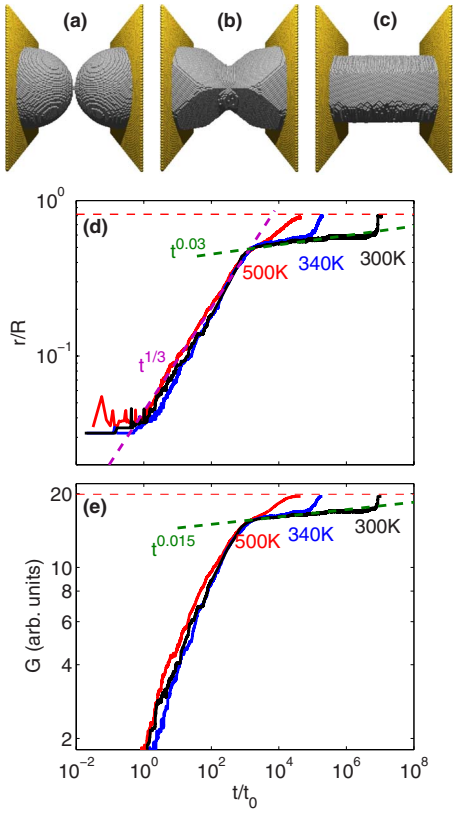

FIG. 6. (Color online) Results of KMC simulations. [(a)–(c)] Neck of two neighboring half-cluster ($R=20$ lattice constants, $E_0=0.17$ eV) at $T=300$ K with periodic boundary conditions at times $t/t_0=0,10^4,10^7$. Vertical planes allow the boundaries to be visualized. The system evolves from two half-spheres connected by one atom at $\frac{t}{t_0}=0$: to a facetted cylinder at $\frac{t}{t_0}=10^7$ through a facetted transition state at $\frac{t}{t_0}=10^4$. [(d) and (e)] Evolution of the neck radius and conductance assuming dominant bulk scattering for $T=300$, 340, and 500 K starting from the configuration shown in (a).

KMC simulations, using a bond-counting model,[23,24] were previously used to model the coalescence of unsupported cluster pairs.[22] We have utilized the same model to simulate the coalescence of several clusters in many geometries, including symmetric and asymmetric structures and estimated their electrical conductance. The key results are well illustrated by a pair of "half clusters" of radius R, with periodic boundary conditions [see Figs. 6(a)–6(c)]. Obviously these simulations cannot model the experiments in a precise way because of the different crystal structures, cluster size, and possible substrate interactions; nevertheless, the general features of the coalescence process are not expected to depend strongly on these parameters.

Figures 6(a)–6(c) shows the evolution of the neck at 300 K, taking the energy of a single bond $E_0=0.17$ eV, which corresponds to the cohesive energy of Bi and is comparable to values found from molecular-dynamics simulations of gold nanoparticles.[25] The system evolves from two half-spheres to a faceted cylinder through a late stage characterized by a well-defined shape where atomic planes are clearly visible. The apparent "freezing" of the evolution is linked with the formation of highly stable atomic facets.[22,23] The evolution of the neck radius is shown in Fig. 6(d). As previously observed for a pair of free clusters,[22] Eq. (1) is obeyed for $r<\frac{R}{2}$ with $\alpha=\frac{1}{3}$. After this initial increase, it is observed that there is a much slower period of neck evolution with $\alpha=0.03$ for a length of time that depends on the temperature. Eventually r increases to the cylinder radius. The slow evolution of the neck radius, and the small value of α, is consistent with molecular-dynamics simulations of an unsupported pair of Au clusters.[21]

As for metallic wires, the electrical conductance will be determined by three physical processes: bulk, grain boundary, and surface scattering.[26,27] The dominant process depends on the ratio between the electron mean-free path λ and the size of the wire and the grains. The conductance of the two half-clusters was calculated for the three extreme cases (i.e., where one process dominates the two others). Throughout the late stage of the coalescence, we find that in all three cases $G(r)$ obeys a power law. Hence, even though $\frac{r}{R}$ is not small, Eq. (2) still can be used and ω has a well-defined value. First, if bulk scattering is dominant, $\omega=\frac{1}{2}$, and $G(t)$ follows $t^{0.015}$ [see Fig. 6(e)], hence $\beta=0.015$. Second, if grain boundary scattering is dominant, and as the clusters are monocrystalline,[28] the only grain boundary is at the interface between the two clusters, we find $\omega=2$ and $\beta=0.06$. Finally, when surface scattering is the dominant process, we find $\omega=1$ and $\beta=0.03$. Similar results are obtained from numerical treatment of the continuum surface diffusion problem for coalescing particles.[29]

Hence, the KMC simulations show that a late stage of very slow neck radius evolution exists at low temperature for $\frac{r}{R}\geq 0.5$ and that during this stage the conductance follows a power law in time, with an exponent β between 0.015 and 0.06. This is very close to the exponent determined above for the experimental cluster film ($\beta\sim 0.02$), and strongly suggests that the evolution in conductance observed in the experimental cluster films corresponds to this late stage of coalescence. On a quantitative level, and recalling that $\beta=\alpha\cdot\omega$, this experimental value of β corresponds to $0.01\lesssim\alpha\lesssim 0.04$.

In summary, we have observed experimentally that the conductance of a Bi cluster *film* follows a power law in time. Our simulations of percolating films show this is consistent with a power-law evolution of the conductance *between clusters*. The power-law exponent β is determined to be ~ 0.02, and hence the power-law exponent governing the evolution of the neck radius in Eq. (1) is $\alpha\lesssim 0.04$. This value of α is much smaller than expected from continuum theory ($\alpha=\frac{1}{6}$) but is consistent with observations of small power-law exponents in simulations of later stages in the coalescence process. We believe that predicted[2,3] large exponents $\alpha\sim\frac{1}{6},\frac{1}{3}$ are not observed in the experiments because they occur on a time scale much faster than the experiments (Fig. 6 shows that the late stage processes occur over very much longer time scales). While, experimentally, some clusters are clearly faceted (Fig. 3 and Ref. 28), resolution limitations preclude a detailed investigation of the structure of the neck regions. Nevertheless, the present results are consistent with experimental studies[8] and simulations[21,22] which demonstrate the importance of faceting near the necks.

[1] L. Rayleigh, Proc. London Math. Soc. **s1-10**, 4 (1878).
[2] G. C. Kuczynski, J. Appl. Phys. **20**, 1160 (1949).
[3] F. A. Nichols and W. W. Mullins, J. Appl. Phys. **36**, 1826 (1965).
[4] C. Herring, J. Appl. Phys. **21**, 301 (1950).
[5] M. E. Toimil Molares, A. G. Balogh, T. W. Cornelius, R. Neumann, and C. Trautmann, Appl. Phys. Lett. **85**, 5337 (2004).
[6] J. Schmelzer, S. A. Brown, A. Wurl, M. Hyslop, and R. J. Blaikie, Phys. Rev. Lett. **88**, 226802 (2002).
[7] W. D. Kingery and M. Berg, J. Appl. Phys. **26**, 1205 (1955).
[8] T. H. Lim, D. McCarthy, S. C. Hendy, K. Stevens, S. A. Brown, and R. D. Tilley, ACS Nano **3**, 3809 (2009).
[9] M. Massachi, J. Appl. Phys. **48**, 1408 (1977).
[10] A. Mikrajuddin, F. G. Shi, H. K. Kim, and K. Okuyama, Mater. Sci. Semicond. Process. **2**, 321 (1999).
[11] T. Schulze, J. Comput. Phys. **227**, 2455 (2008).
[12] B. Weitzel and H. Micklitz, Phys. Rev. Lett. **66**, 385 (1991).
[13] Y. M. Lin, S. B. Cronin, J. Y. Ying, M. S. Dresselhaus, and J. P. Heremans, Appl. Phys. Lett. **76**, 3944 (2000).
[14] P. Hofmann, Prog. Surf. Sci. **81**, 191 (2006).
[15] R. Reichel, J. G. Partridge, A. D. F. Dunbar, S. A. Brown, O. Caughley, and A. Ayesh, J. Nanopart. Res. **8**, 405 (2006).
[16] D. Stauffer and A. Aharony, *Introduction to Percolation Theory* (Taylor & Francis, London, 1992).
[17] J.-M. Wen, J. W. Evans, M. C. Bartelt, J. W. Burnett, and P. A. Thiel, Phys. Rev. Lett. **76**, 652 (1996).
[18] C. T. Campbell, Surf. Sci. Rep. **27**, 1 (1997).
[19] P. Y. Convers, A. Sattar, S. C. Hendy, and S. A. Brown (unpublished).
[20] A. Clauset, C. R. Shalizi, and M. E. J. Newman, SIAM Rev. **51**, 661 (2009).
[21] L. J. Lewis, P. Jensen, and J.-L. Barrat, Phys. Rev. B **56**, 2248 (1997).
[22] D. N. McCarthy and S. A. Brown, Phys. Rev. B **80**, 064107 (2009).
[23] N. Combe, P. Jensen, and A. Pimpinelli, Phys. Rev. Lett. **85**, 110 (2000).
[24] P. Jensen and N. Combe, Comput. Mater. Sci. **24**, 78 (2002).
[25] F. Baletto, C. Mottet, and R. Ferrando, Surf. Sci. **446**, 31 (2000).
[26] R. B. Dingle, Proc. R. Soc. London, Ser. A **201**, 545 (1950).
[27] A. F. Mayadas and M. Shatzkes, Phys. Rev. B **1**, 1382 (1970).
[28] K. J. Stevens, K. S. Cheong, D. M. Knowles, N. J. Laycock, A. Ayesh, J. Partridge, S. A. Brown, and S. C. Hendy, Curr. Appl. Phys. **6**, 453 (2006).
[29] S. C. Hendy (unpublished).